

# Multi-Resolution Local Binary Pattern for Assessing Cervical Ripening

Pablo J. Vázquez Obando<sup>1,2</sup>, Nestor Arana A.<sup>1</sup>, and Alberto Izaguirre<sup>1</sup>

<sup>1</sup>Mondragon University, Basque Country, Spain

<sup>2</sup>National University of Engineering, Nicaragua

Email: pablo.vasquez@alumni.mondragon.edu, {narana, aizagirre}@mondragon.edu

Jorge Burgos and Itziar Arana

Obstetrics and Gynecology Service BioCruces Health Research Institute, Spain

Email: jburgoss@sego.es

**Abstract**—Labor induction is defined as the artificial onset of labor for the purpose of vaginal birth. Cesarean section is one of the potential risk of labor induction as it occur in about 20% of the inductions. A ripe cervix (soft and distensible) is needed for a successful labor. During the ripening cervical tissues experience micro structural changes: collagen becomes disorganized and water content increases. It is expected that these changes will affect the interaction between cervical tissues and the sound waves during ultrasound transvaginal scanning and will be perceived as gray level intensity variations in the echographic image. Texture analysis can be used to analyze these variations and provide a means to evaluate cervical ripening in a non-invasive way. In this paper we analyze a set of Transvaginal Ultrasound (TVU) images using a multiresolution Local Binary Pattern to study their textures for classification purposes.

**Index Terms**—texture analysis, local binary pattern, cervical ripening, ultrasound imaging

## I. INTRODUCTION

Labor induction carries various risks, including: cesarean section, intrapartum fetal heart rate alterations, infections, fetal acidosis, and postpartum hemorrhage. Nowadays in Spain about 30% of deliveries are induced and about 20% [1] end in cesarean section.

It is likely that some of these unwanted outcomes result from intervening when the uterus and cervix are not ready for labor. For this reason the evaluation of cervical ripening is a crucial step when planning a labor induction procedure.

At present, the only standard method for predicting the chance of successful labor induction and determining the induction protocol consists of digital examination to assess spontaneous cervical ripening, usually indicated by the Bishop score. This method being manual is subjective and prone to errors and inter observer variability.

A more accurate evaluation of cervical ripening is desirable prior labor induction process is started. It is known that the cervix tissues goes through remarkable

changes along pregnancy. Collagen, the most abundant element in the cervical micro structure (about 85%) is aligned and organized in the cervix of non-pregnant women and displayed progressively more disorganized during remodeling of the cervix as the pregnancy progresses in preparation for the delivery [2]. Besides collagen changes, water content of the cervical tissues is also increased.

The aforementioned changes in cervical microstructure and tissue hydration are expected to give raise to changes in the image obtained from Transvaginal Ultrasound (TVU) since the consistency of tissues affect their interaction with the sound waves.

In this research work, we explore image processing algorithms capable to assess cervical changes based on transvaginal ultrasound B-mode images for predicting the risk of cesarean section. The importance of these tools lies in that they could influence the clinical management of induction of labor and the reduction in the cesarean rate.

## II. PATIENTS AND DATA

Pregnant women currently referred to the Cruces University Hospital (Bilbao, Spain) for labor induction, constitute our patient database for study. Singleton pregnancies, head-first presentation and  $\leq 37$  weeks of gestation were the inclusion criteria. Pregnancies of fetus suffering from infections and abnormalities were not included. A set of 82 patient data were included in this study.

Annotations about weeks of pregnancy, labor induction reason and labor outcome were also attached to the collected images. Setting for the ultrasound scanner were defined in a protocol and practiced for all obstetricians participating in this study. Images were acquired during routine patient transvaginal scanning prior to labor induction.

Labor induction process is usually divided into two stages: A 24 hours ripening stage where prostaglandins are administered, followed by a 12 hours stimulation stage where the treatment is oxytocin in case cervical ripening is not achieved.

Thus a successful ripening is defined when a Bishop Score >6 is obtained within 24 hours after induction is started. Labor induction failure is considered when after 36 hours the cervix still has a Bishop Score ≤6.

A total of 82 DICOM files were acquired, and from these 60 belong to patient with a vaginal delivery and 22 to cesarean section as detailed in Table I. All images in the database included two ROIs.

TABLE I. PATIENTS DATABASE

	Ripening Stage	
	Vaginal delivery	Cesarean Section
RS	50	11
RF	1	0
TS	3	1
<b>Total</b>	54	12
	Stimulation Stage	
	Vaginal delivery	Cesarean Section
SS	6	6
SF	0	2
FWBR	0	2
<b>Total</b>	6	10

Legend: RS=ripening successful, RF = ripening failure, TS = Tachysystole, FWBR = Fetal Well-Being at Risk, SS= Stimulation successful, SF: Stimulation failure

These ROIs were manually delineated by an expert obstetrician and defined the border of cervix lips (see Fig. 1).

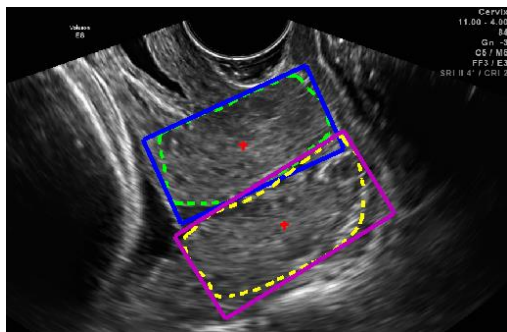


Figure 1. A sample Transvaginal Ultrasound image with two ROIs manually delineated corresponding to the anterior and posterior cervical lips.

### III. ULTRASOUND IMAGING

Extracting useful information from Ultrasound (US) B-mode images is a challenging task. US images are low contrast, contain blurred edges and they are normally contaminated with speckle noise. Despite these drawbacks a lot of effort has been made on processing US images. The main reason is the attractive characteristic of clinical ultrasound: a non-invasive, non-ionizing and relatively low cost medical image modality.

Texture is an important property of images. Although not yet defined texture is related to patterns and changes on brightness on an image. In US imaging we talk about echogenicity to refer to the gray level in the image, thus an echogenic region means brighter region. These changes of luminance constitute texture.

Texture has been used in many topics of image analysis. For example it has been successfully used for organ segmentation as in [3] for liver segmentation, kidney [4] and prostate [5] or for tissue classification task where the goal is to differentiate from healthy and abnormal tissue. Some classification examples are shown in [6] on liver, breast [7] or cervix [8].

One important aspect of texture is scale. It is known that human visual system processes images in a multi-scale way. The visual cortex has separate cells that respond to different frequencies and orientations. Analyzing texture at different resolutions is required when dealing with non-stationary textures as those obtained in medical imaging.

#### A. Wavelets

A wavelet is a mathematical function used to divide a given function or continuous-time signal into different scale components. Usually one can assign a frequency range to each scale component. Each scale component can then be studied with a resolution that matches its scale. A wavelet transform is the representation of a function by wavelets. The wavelets are scaled and translated copies of a finite-length or fast-decaying oscillating waveform (known as the mother wavelet).

Wavelets have been used extensively since its development. In image processing wavelets have become popular tools for denoising, compression and enhancement. For texture classification we can mention [9], [10], analysis of medical images for Computer Tomography [11] and prostate evaluation [12].

We tested one of the most utilized texture descriptors, the Local Binary Pattern (LBP) in a multi resolution fashion.

#### B. The Local Binary Pattern (LBP)

The LBP operator, introduced by Ojala *et al.* has been shown to be a powerful measure of image texture [13]. As a texture descriptor it has been found useful in many medical applications. For instance, image segmentation [14] medical image retrieval [15] and ulcer detection [16].

In its original form, the operator works by thresholding a 3×3 neighborhood with the value of the center pixel, thus forming a local binary pattern, which is interpreted as a binary number. The occurrences of different local patterns are collected into a histogram that is used as a texture descriptor. By definition LBP is invariant to any monotonic gray-scale transformation

The LBP texture unit is calculated in a 3×3 square neighborhood by applying a simple threshold operation with respect to the central pixel as illustrated in (1).

$$T = t(g_o - g_c), \dots, (g_{p-1} - g_c)$$

$$t(x) = \begin{cases} 1 & \text{if } x \geq 0 \\ 0 & \text{if } x < 0 \end{cases} \quad (1)$$

where  $T$  is the texture unit,  $g_c$  is the grey level value of the central pixel,  $g_p$  are the grey level values of the pixels adjacent to the central pixel in the 3×3 neighborhood,  $P$  defines the number of pixels in the 3×3 neighborhood and function  $t(\cdot)$  defines the threshold operation.

For a  $3 \times 3$  squared neighborhood the value of P is 8. To encompass the spatial arrangement of the pixels in the  $3 \times 3$  neighborhood, the LBP value for the tested (central) pixel is calculated using the following relationship:

$$LBP = \sum_{i=0}^{P-1} t(g_i - g_c) 2^{-i} \quad (2)$$

where  $t(g_i - g_c)$  is the value of the thresholding operation illustrated in (1). The LBP values calculated using (1) are in the range  $[0, 255]$ .

Several variants have been introduced that modify some aspects of the original LBP. For example different shapes for the neighborhood have been proposed. Circular, elliptical, parabolic, hyperbolic [17] and radii larger than one, which requires interpolation of points not on pixel locations. Also the original binary encoding has been replaced by ternary or even quinary encoding. Some samples of circular LBP neighborhood are shown in Fig. 2.

Additionally since the original LBP was not rotation invariant the so-called uniform patterns have been developed. These are special patterns with at most two transitions.

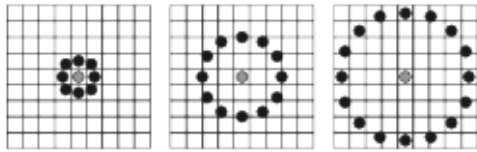


Figure 2. Different resolution LBPs using a circular neighborhood. Left P=8, R=1, Center: P=12, R=1.5 and left P=16, R=4

#### IV. PREVIOUS RESEARCH

In previous publications on texture analysis of cervical tissue, mainly related to preterm birth risk assessment, it has been found that some statistical parameters change in response to cervical ripening. These parameters were mainly derived from gray level histograms and co-occurrence matrices. According to [18], the brightness of the texture decreases in the area of the external os (external opening of the cervix) from the state of non-pregnancy to early and late pregnancy. In the area of the inner os (internal opening) the contrast increases and homogeneity decreases; in the external os area texture changes are the opposite. The textures in the area of the internal os of pregnancies complicated by preterm labor were dark, showed more contrast and less homogeneity compared to term pregnancies.

In [19] it was found that a more echogenic anterior than posterior cervix indicates a hard cervix; the greater the difference in echogenicity between anterior and posterior walls the harder the cervix. These findings allow us to expect a good tissue classification using texture derived parameters,

#### V. METHODOLOGY

##### A. Image Acquisition and Pre-Processing

All images were acquired with a Voluson E8 Ultrasound scan scanner from General Electric. For the

analysis of the cervical tissue we followed the sequence shown in Fig. 3.

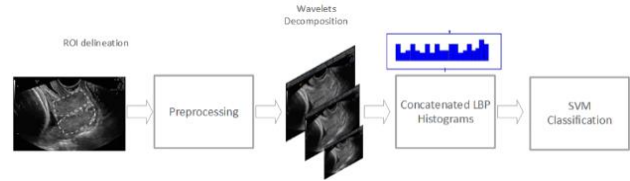


Figure 3. The different steps in the multiresolution methodology for LBP analysis of TVU images.

First, rectangular sections containing each of the ROIs were cropped automatically from the original gray level images using code written in Matlab and OpenCV. These rectangles are minimal in the sense that they are the smallest containing the ROI points and have arbitrary orientation to minimize the amount of non ROI pixels included (see Fig. 1).

Normalization of the images was performed by the 3-sigma method in which all pixels in an image are restricted to be within the interval  $\mu \pm \sigma$  where  $\mu$  is the mean gray value and  $\sigma$  is the standard deviation.

##### B. Multiresolution Scheme

To allow for multi-resolution, the image is first decomposed in a pyramidal way using the wavelets transform. The *Daubachies IV* wavelets was utilized for decomposition. Only the approximation image was processed in this work. The LBP operator is applied to the different scale version of the image and then the histograms calculated from each resolution are concatenated to form a combined histogram.

In our implementation for the multi-resolution LBP, the neighborhood size was set to  $P = 4, 6, 8$  or  $16$ , we let  $R=1$  for all calculations since the resolution is changed by down-sampling operations carried out by the wavelets transform. We tried three different mapping for the LBP, uniform ('u2'), rotation invariant ('ri') and uniform-rotation invariant ('riu2') as described in [18]

##### C. Data Preprocessing

It was found in the experiments that the performance of the classifier improves if the histograms were normalized to be zero mean and unit variance.

##### D. Classification

The support vector machine classifier was used for classification. A Gaussian kernel was set for the SVM with a cost parameter of 0.8.

We performed two types of classifications:

- One classification using four models, one for each cervical lip (L1 anterior, L2 posterior) of two classes ('Vaginal', 'Cesarean'). i.e. "VL1", "VL2", "CL1", "CL2".
- Classification of the cervix image using one model for each class.

The first classification scheme was intended to study if the anterior and posterior lips show meaningful differences for each class because according to the previous works there are differences in the echogenicity of both lips.

For error calculation we performed k-fold cross-validation on our dataset, with k = 8, 10 and 12 folds.

### VI. RESULTS

All cases were organized into 3 categories depending on the relationship with cervical ripening (Table II).

TABLE II. CASES CLASSIFICATION

Category	Cesarean Section reason
High	Labor induction failure
Medium	Secondary Arrest of Dilatation
Low /Null	Breech Presentation

A total of 54 files were used during classification experiments. The data set was divided into two groups one containing the patients with delivery within 24 hours (ripening success) and 36 hours, i.e. those with stimulation stage and including only cases from high and medium category.

Results for the first group (43 images) are summarized as follows:

- a) For the individual lip models, we obtained 88.9%, 88.9%, 66.7% and 0% of correct identification for VL1, VL2, CL1, CL2. This might suggest that the anterior lip possesses more discriminant texture attributes.
- b) For the global model, results are summarized in Table III.

As shown, the best classification performance was achieved by using the 'riu2' mapping. For the case P=16 the performance decreases again, thus P=8 is considered optimum.

TABLE III. CLASSIFICATION RESULTS (AUC)

Mapping	P=4	P=6	P=8
riu2	0.83333	0.87037	<b>0.90741</b>
u2	0.72222	0.72222	0.7037
ri	0.83333	0.7963	0.66667

Area under the curve (AUC) parameters obtained using the different mappings for the LBP.

### VII. DISCUSSION

In this paper we analyzed a set of TVU images from the cervix by means of a multi-resolution LBP scheme using wavelets for pyramidal decomposition

Results show that apparently the anterior lip of the cervix experience more echogenicity changes through the ripening process. This is probably due to the fact that the anterior lip is normally the first in the path of the ultrasound beam, this causes that when a hard cervix is analyzed the posterior lips receives less ultrasound power.

The percentage of good classification for the first group was 82%, a ROC curve for this group is shown Fig. 4. When including the cases of the second category the performance decreases to almost 77%.

The cervical tissue classification by means of texture has the potential to become a great tool for cervical ripening assessment.

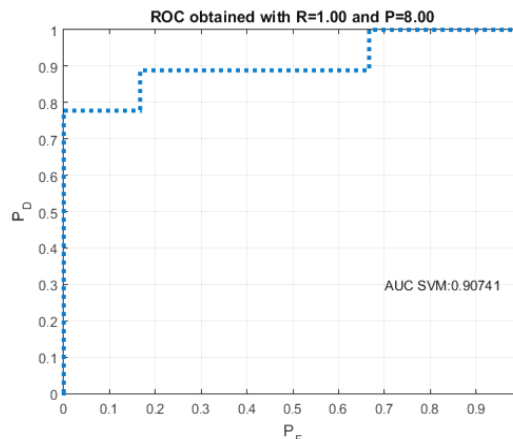


Figure 4. ROC curve for P=8 and LBP with uniform rotation invariant mapping and the 24 hours group.

### ACKNOWLEDGMENT

The authors would like to thank to our counterparts at the Obstetrics and Gynecology Service, BioCruces Health Research Institute for their collaboration and advice related to clinical perspective of the provided data.

### REFERENCES

- [1] F. S. Molina and K. H. Nicolaidis, "Ultrasound in labor and delivery," *Fetal Diagn. Ther.*, vol. 27, no. 2, pp. 61-67, 2010.
- [2] H. Feltovich and T. J. Hall, "Quantitative imaging of the cervix: Setting the bar," *Ultrasound Obstet. Gynecol.*, vol. 41, no. 2, pp. 121-128, Feb. 2013.
- [3] S. Milko, E. Samset, and T. Kadir, "Segmentation of the liver in ultrasound: A dynamic texture approach," *Int. J. Comput. Assist. Radiol. Surg.*, vol. 3, no. 1-2, pp. 143-150, May 2008.
- [4] C. H. Wu and Y. N. Sun, "Segmentation of kidney from ultrasound B-mode images with texture-based classification," *Comput. Methods Programs Biomed.*, vol. 84, no. 2-3, pp. 114-123, 2006.
- [5] H. Ladak, F. Mao, and Y. Wang, "Prostate boundary segmentation from 2D ultrasound images," *Med. Phys.*, vol. 27, no. 1777, 2000.
- [6] K. R. Sudhakar and R. Sudhakar, "Automatic classification of liver diseases from ultrasound images using GLRLM texture features," *Soft Comput. Appl.*, pp. 611-624, 2013.
- [7] I. Muhimmah and R. Zwigelaar, "Mammographic density classification using multiresolution histogram information," in *Proc. International Special Topic Conference on Information Technology in Biomedicine*, 2006.
- [8] Q. Ji, J. Engel, and E. Craine, "Texture analysis for classification of cervix lesions," *IEEE Trans. Med. Imaging*, vol. 19, no. 11, pp. 1144-1149, Nov. 2000.
- [9] A. Busch and W. Boles, "Texture classification using multiple wavelet analysis," in *Proc. Sixth Digital Image Computing Techniques and Applications Conference*, 2002, pp. 341-345.
- [10] A. Ahmadian and A. Mostafa, "An efficient texture classification algorithm using Gabor wavelet," in *Proc. 25th Annu. Int. Conf. IEEE Eng. Med. Biol. Soc.*, 2003.
- [11] L. Semler, L. Dettori, and J. Furst, "Wavelet-Based texture classification of tissues in computed tomography," in *Proc. 18th IEEE Symposium on Computer-Based Medical Systems*, 2005, pp. 265-270.
- [12] K. Jafari-Khouzani and H. Soltanian-Zadeh, "Multiwavelet grading of pathological images of prostate," *Biomed. Eng. IEEE Trans.*, vol. 50, no. 6, pp. 697-704, 2003.
- [13] T. Ojala, M. Pietikäinen, and T. Mäenpää, "Multiresolution gray-scale and rotation invariant texture classification with local binary patterns," *IEEE Trans. Pattern Anal. Mach. Intell.*, vol. 24, no. 7, pp. 971-987, 2002.
- [14] T. Ojala and M. Pietikäinen, "Unsupervised texture segmentation using feature distributions," *Pattern Recognit.*, vol. 32, no. 3, pp. 477-486, 1999.

- [15] C. Christiyana and V. Rajaman, "Comparison of local binary pattern variants for ultrasound kidney image retrieval," *Int. J. Adv. Res. Comput. Sci. Softw. Eng.*, vol. 2, no. 10, pp. 224-228, 2012.
- [16] B. Li and M. Meng, "Texture analysis for ulcer detection in capsule endoscopy images," *Image Vis. Comput.*, vol. 27, no. 9, pp. 1336-1342, 2009.
- [17] L. Nanni, A. Lumini, and S. Brahnam, "Local binary patterns variants as texture descriptors for medical image analysis," *Artif. Intell. Med.*, vol. 49, no. 2, pp. 117-125, Jun. 2010.
- [18] H. Jörn, K. Kalf, W. Rath, R. Copyright, E. Creativity, and H. Jörn, "Prediction of premature birth using texture analysis of the cervix," *Ultraschall der Medizin-European J. Ultrasound*, vol. 29, no. OS2, p. PO16, 2005.
- [19] T. Kuwata and S. Matsubara, "A novel method for evaluating uterine cervical consistency using vaginal ultrasound gray-level histogram," *J. Perinat. Med.*, vol. 38, no. 5, 2010.



– Multiscale methods.

**Pablo J. Vázquez** received his title on Electrical Engineering in 1994 from National University of Engineering at Managua, Nicaragua. He also received the degree of Licentiate of Engineering in Biomedical Signal Processing from Lund University of Technology (Lund, Sweden). Currently he is involved in a doctorate program at Mondragon University, Spain. His research interests are Medical Image Processing by Multiresolution